Leader-Follower Systems with Sensor Integration

Jiajun Guo 2522597 Dongqing Shao 2522930 Xinhui Li 2425886

***Abstract*—This study evaluates the optimal combination of line sensors and bump sensors on the Pololu 3pi+ robot. It focuses on improving signal detection, tracking stability, and response time in various motion scenarios, including constant speed, variable speed, and sudden turns. The optimal performance was achieved through the fusion of the middle three line sensors and the left bump sensor in all motion scenarios. The experiment yielded a signal detection accuracy of over 99%, with a system response time of approximately 400 milliseconds. The data indicated that sensor fusion is an effective method for handling sudden changes in speed or direction during leader-follower tasks.**

I. Introduction

Leader-follower tasks are widely used in autonomous vehicle formation, cooperative multi-agent systems and other fields. Early studies mainly performed detection by using a single sensor, such as vision-based tracking, where a camera was used to detect and track the target robot, but suffered from the difficulties of computational complexity and sensitivity to changes in lighting conditions [1], [2]. Hence, researchers considered infrared (IR) sensors to address these limitations because they are reliable and computationally inexpensive, especially in close-range detection [3]. Recent studies have demonstrated the advantages of multisensor systems [4], by combining ultrasonic and infrared sensors to show improved tracking and obstacle avoidance performance using the complementary advantages of sensors [5]. Leader-Follower tasks require precise control and powerful sensor integration to achieve effective following behavior [6], and the Pololu 3pi+ robot platform, equipped with five line sensors and two bump sensors, provides the ideal environment to explore the challenges of such tasks [7].

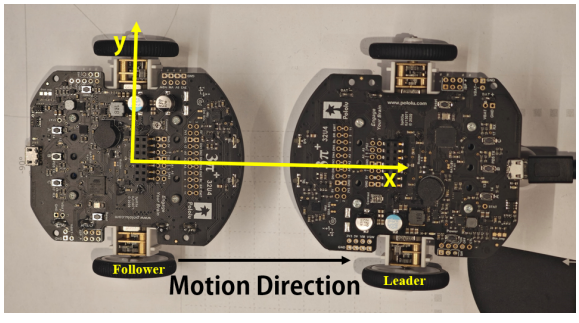

Fig. 1. The Pololu 3pi+ Robots Used in Experiments

Maintaining consistency of relative positions between two robots is of great importance in leader-follower systems. The follower robot must accurately detect and respond to the leader's movements in order to guarantee an optimal distance while adapting to changes in direction and velocity. In the Pololu 3pi+ robot system (Fig. 1), five line sensors and two bump sensors are available for use. However, not all sensors on the robots are sufficiently sensitive to maintain the optimal distance. The line sensors can detect infrared reflections from the surface, providing high spatial resolution for tracking. However, they may cause tracking errors when the direct infrared signals from the leader are weak. While bump sensors are more suitable for detecting short-range infrared signals, their spatial resolution remains limited. Furthermore, the left bump sensor (BL) is only compatible with analogue-to-digital converter (ADC) readings, whereas the right bump sensor (BR) is only compatible with digital readings [8].

By selectively using some or all of the sensors, the optimal sensor configuration for performing the following task can be determined. The deployment of a reduced number of sensors effectively reduces the hardware demands on the robot, thereby providing sufficient resources to support the implementation of complex program designs. The selected sensor combinations will be tested under three conditions: constant speed linear motion, variable speed linear motion, and constant-speed sudden turn motion. The evaluation criteria will focus on positional deviation and the response time delay between the follower robot and the leader robot.

A. Hypothesis Statement

The line sensor provides precise spatial resolution and orientation information, making it suitable for detecting and tracking the trajectory of the leader robot, especially during sudden orientation changes. While the bump sensor provides reliable intensity measurements ensuring effective signal detection at close range and enhancing tracking performance during linear motion. We hypothesize that the combination of line sensors and bump sensors will provide better performance for Leader-Follower tasks than either type of sensor alone. Specifically, we propose the following hypotheses:

> *It is hypothesized that "the combination of line sensors and bump sensors on the Pololu 3pi+ robot enables better signal detection, higher following stability, and faster response time in Leader-Follower tasks than using only a single sensor.*
>
> *It is further assumed that when the leader suddenly turns, the signal of the outermost linear sensor may be lost, and the following robot can make a fast response by ensuring stable signal detection through the middle three linear sensors, while the bump sensor will ensure reliable signal detection in linear motion.*

The remainder of this paper is systematically organised as follows. Section II introduces the system we designed and used. Experiment Procedures and evaluation methods are discussed in section III. Section IV presents the experimental results. Section V evaluates the results and provides a comprehensive conclusion.

II. Implementation

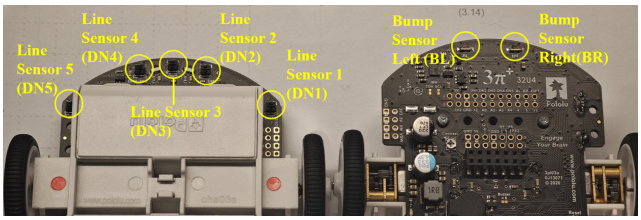

Fig. 2. Sensor Distribution in Pololu 3pi+ Robot System

To the aforementioned hypotheses, the implementation of this experiment is as follows: In this experiment, two Pololu 3pi+ robots were used as the test platform, utilizing the line sensors and bump sensors on the robots, shown in Fig. 2. Five line sensors are positioned at the front of the robot, facing downward. From left to right, they are: Line Sensor 1 (DN1, leftmost), Line Sensor 2 (DN2, mid-left), Line Sensor 3 (DN3, middle), Line Sensor 4 (DN4, mid-right), and Line Sensor 5 (DN5, rightmost). There are also two forward-facing bump sensors in the front of the robot. The Arduino integrated development environment (IDE) is used to implement the software, and all experimental data are obtained through its Serial Monitor. The program consists of three main parts: sensor initialisation and calibration, distance detection and evaluation, and speed control using PID. In light of the inherent limitations of the robot system's hardware, the implementation concentrates on the acquisition of hardware data and its display within the software component.

Algorithm 1 Follower Robot Control Process

Input: Sensor readings, encoder values
Output: Robot motion control

Initialise hardware pins, motors, sensors, and encoders
$pose \leftarrow$initialise(0, 0, 0)
$cali\_f \leftarrow 1$
$currentRecord \leftarrow 0$
$timestamp \leftarrow millis()$
while true **do** ▷ Main Loop
  $leftBumpValue \leftarrow$ `analogRead`
  $rightBumpValue \leftarrow$ `digitalRead`
  $linesensor \leftarrow$ `analogRead`
  if $millis() - time\_flag > 200$ **then**
    for $i \leftarrow 0$ to $numSensors - 1$ **do**
      $sensorData[currentRecord][i]$
    end for
    Serial.println("currentRecord:")
    $time\_flag \leftarrow millis()$
  end if
  if $cali\_f = 5$ **then**
    `speed_detect()`
    `speed_control()`
  else
    `Calibration_bump_line()`
  end if
  Delay(10)
end while

The pseudo-code shows the control process of the follower. The hardware involved in the initialisation and calibration process includes motors and encoders, an inertial measurement unit (IMU), line sensors, and bump sensors. Through the calibration procedure, the reading range of the line sensor and bump sensor can be obtained in the current environment, so that the follower can steadily track the leader in different environmental conditions. Specifically, bump sensors determine distance extrema by rotating in place near the leader, while line sensors identify distance extrema by moving closer to or farther away from the leader, thereby enhancing the effectiveness of the following task. In addition, the infrared emitters of the line sensor and the bump sensor are controlled by the same pin labelled EMIT, driving this pin at a high power level, the line sensor emitters emit light, while driving it at a low power level activates the bump sensor emitters [8]. Consequently, the experiment was conducted to evaluate the efficacy of the EMIT pin configurations, ultimately determining that maintaining a high-level output state was optimal. In this configuration, both sensor types operate as intended, thereby enabling effective sensor fusion.

Once the calibration process is complete, the robot will enter the distance detection and evaluation process. The follower will establish an effective reading range for the sensor by using the extreme value data stored during the calibration process, then divide the range into several percentage segments, so that the follower robot can continuously collect sensor data and compare the current value with the segmented threshold. This not only filters out any incidental environmental or system noise, but also estimates the distance between the leader and follower, thereby guiding speed control.

Finally, regarding speed control, the conversion between speed and distance is achieved through the encoder counts on the wheels. By adjusting parameters, this study associates the encoder readings with the Pulse Width Modulation (PWM) speed. As a result, when the distance changes, the current following speed is calculated, and appropriate acceleration or deceleration adjustments are made. With the distance evaluation by the robot platform, this study initially decided to implement stepwise velocity changes for different distances. Given that sudden changes in velocity can result in fluctuations in the distance evaluation, proportional-integral-derivative (PID) was implemented to achieve a smooth transition in velocity. Moreover, the velocity alteration may appear considerable when the distance variation is minimal, particularly in proximity to the thresholds. Therefore, this study plans to employ a machine learning approach to obtain speed data at different distances. With the help of a serial monitor, an approximate distance-to-speed equation is fitted, allowing the required speed to be calculated using only the current distance information.

This study conducted three experiments to verify the effectiveness of sensor fusion in sudden turn motion. All three experiments followed the same procedure described above. However, the first and second experiments used only a single type of sensor—either line sensors or bump sensors—while the third experiment utilised both types of sensors simultaneously.

III. Experiment Methodology

The experiment aims to evaluate the performance of the Pololu 3pi+ robot's sensor configurations in the Leader-Follower task. This section introduces the experimental setup, variables, and procedures, focusing on reproducibility and systematic evaluation. The methodology is described in the flowchart shown in Fig. 3.

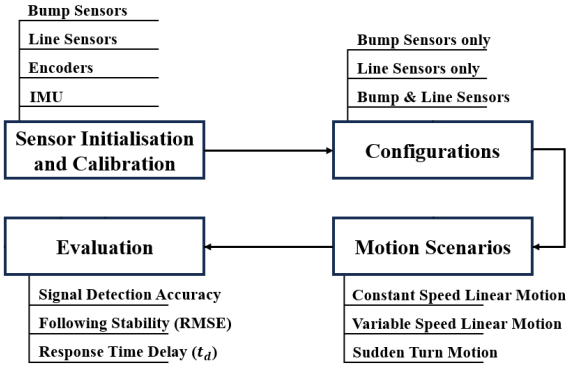

Fig. 3. Methodological Flow Chart

A. Overview of Method

1) The experiment involved three main sensor configurations:
   - Single sensor: The follower uses only two forward-facing bump sensors or only five downward-facing line sensors.
   - Sensor combination: The follower simultaneously uses two forward-facing bump sensors and five downward-facing line sensors.
   - Best sensor combination for sudden turns: The follower uses a combination of the Bump Sensor LEFT (BL), the Line Sensor 2 (DN2, mid-left), the Line Sensor 3 (DN3, middle), and the Line sensor 4 (DN4, mid-right).
2) For each configuration, an initial test is conducted to determine the optimal following distance d:
   - The follower robot is stationary at the starting position, while the leader robot moves in a liner at a constant speed of 15 towards the follower until the two robots collide headon. During this process, the sensor data of the follower robot is recorded and the sensor reading characteristics are observed.
3) Each configuration is tested in three scenarios:
   - Constant Speed Linear Motion: The leader moves straight with a constant PWM set to 15.
   - Variable Speed Linear Motion: The leader moves in a straight line and the speed varies at 15 PWM and 20 PWM every 5 seconds.
   - Sudden Turn Motion: During movement, the leader suddenly turns about 45 degrees, then continues moving straight in the new direction at a constant PWM of 15.
4) For each case, the performance of the following robot is measured by maintaining an optimal distance d. Data was collected through 10 repeated trials for each configuration and scenario to ensure statistical reliability.

B. Discussion of Variables

To ensure the experiment is well structured and the results are credible, the following key variables are defined:

Independent Variable:

- Sensor Configurations:
  - Bump Sensors Only (BL, BR)
  - Line Sensors Only (DN1, DN2, DN3, DN4, DN5)
  - Sensor combination (2 bump and 5 line sensors)

Dependent Variables:

1) Signal Detection Accuracy (η_{signal}): The ability of the follower's sensors to consistently detect the leader's signal during the test.
2) Position Deviation (ΔP): The coordinates of the Leader and the Follower are represented by (x, y, θ). At the beginning, the coordinates of both robots are $(0, 0, 0)$. The deviation of the positions is calculated by calculating the difference of the coordinates at the end of the two robots. where:
   - x: Movement along the initial robots' direction.
   - y: Movement along the y-axis (perpendicular to the x-axis).
   - θ: Angle of deviation from the initial orientation.
3) Following Stability ($RMSE$): The root mean square error reflects the average deviation in the whole process and is used to evaluate the stability of the following and the degree of trajectory matching.
4) Response Time Delay (t_d): The delay in the follower's adjustment of speed or direction in response to changes in the leader's motion.

Controlled Variables:

1) Environment: The experiment is conducted in a controlled indoor environment with stable ambient light conditions to minimise external infrared interference.
2) Initial Position: The leader and follower start from fixed relative positions, with the follower facing the leader. The initial distance between the robots is set to the optimal distance (d_1, d_2, d_3) determined for each configuration.
3) Operation Duration: The leader and the follower run for 20 seconds in each scenario.
4) Leader motion parameters:
   - Constant Speed Linear Motion: The leader's motor PWM is set to 15.
   - Variable Speed Linear Motion: The motor speed alternates between 15 PWM and 20 PWM every 5 seconds.
   - Sudden Turn Motion: The leader moves straight at a speed of 15, changes direction at the 10th second (counterclockwise or clockwise turns of 45 degrees), and moves straight until the 20th second.

C. Experimental Procedure

Setup:

1) Environment Preparation: The experiment was carried out on a flat, uniform white surface to reduce reflection interference and to ensure uniform light in the experimental environment as much as possible. Markers are placed on the ground to assist in tracking the movement of the robot.

2) Sensor Calibration: The leader and follower robots were placed 2cm apart in the experimental area and the calibration procedure was initiated to obtain the maximum and minimum values for the detection range of the sensors in this environment. The follower first rotates 360 degrees counterclockwise and then 360 degrees clockwise in place at a low PWM of 15 PWM, while the infrared signal strength of the sensor from the two bump sensors is recorded. After the calibration of the bump sensor is completed, the linear sensor is calibrated. The follower robot first moves backward 60mm and then moves forward 50mm. The calibration process detects the infrared intensity under the influence of the environment and the Leader robot to obtain the numerical range of the sensor in the current environment to determine the sensor threshold for later testing.
3) Initial Positioning: After the calibration procedure, the initial posture will be updated. At present, the leader and the follower are located at the starting position, so as to ensure that the follower is aligned with the leader and maintains the corresponding optimal distance d. At this time, the posture of the two robots, that is, the coordinates, are all (0,0,0) in their respective coordinate systems.

Trial Execution:

The test was repeated 10 times for each of the three sensor configurations:

1) The follower's sensor readings are initialised and its range tracking variable is reset to zero.
2) Initiate the actions of the leader according to the defined scenarios: constant speed linear motion, variable speed linear motion or sudden turn motion.
3) Each leader-follower trial lasts 20 seconds.

Data Collection:

For each motion scenario, the test was repeated 10 times for each sensor configuration and the average was taken to ensure statistical reliability. All collected data were saved in structured log files, including timestamps, sensor readings, and motion trajectories for post-experiment analysis. Machine learning was then incorporated into the experiments based on this data.

1) Sensor data: The readings of the Bump sensor and line sensor of the follower, as well as the motor speed of the two robots, are collected and recorded in real time.
2) Trajectory data: Use odometry to get the follower's pose, which is the coordinates x, y, and $theta$.
3) Response time: After detecting a change in the leader, a timestamped adjustment is made to the follower's speed or direction.

D. Metrics for Evaluation

To evaluate the performance of each sensor configuration, the following metrics are used:

1) Signal Detection Accuracy (η_{signal}): The percentage of total runtime during which the follower robot successfully detects the leader's signal. The formula is defined as:

$$\eta_{signal} = \frac{T_{detect}}{T_{total}} \times 100\% \tag{1}$$

where:

- T_{detect} is the total time during which the follower successfully detects the leader's signal.
- T_{total} is the total runtime of the follower robot.

For each test, a follower receiving a valid reading from at least one sensor in each configuration is a successful signal detection. Based on the data obtained in calibration, the maximum and minimum values of each sensor were recorded as Max_i and Min_i, which were used to determine the sensing range of each sensor in the current situation. According to the left bump sensor's readings and the real distance, the optimal tracking distance d_{BL} can be obtained:

$$d_{BL} = (0,\ (\text{Max}_i - \text{Min}_i) \cdot 0.2 + \text{Min}_i) \tag{2}$$

Similarly, when using the line sensor the optimal tracking distance d_L can be obtained:

$$d_L = ((\text{Max}_i - \text{Min}_i) \cdot 0.2 + \text{Min}_i, \\ (\text{Max}_i - \text{Min}_i) \cdot 0.5 + \text{Min}_i) \tag{3}$$

2) Position Deviation (ΔP): The position deviation is used to quantify the coordinate differences between the Leader and Follower at the end of the operation. The calculation formulas are as follows:

$$\Delta P = (x_f - x_l, y_f - y_l, \theta_f - \theta_l) \quad = (\Delta x, \Delta y, \Delta\theta) \tag{4}$$

where:

- x_f, y_f, θ_f are the final coordinates and orientation of the Follower.
- x_l, y_l, θ_l are the final coordinates and orientation of the Leader.

3) Following Stability ($RMSE$): The root mean square error is used to quantify how closely the follower robot maintains its trajectory relative to the leader's path, which is formulated as follows:

$$RMSE = \sqrt{\frac{1}{n}\sum_{i=1}^{n}\left[(\Delta x_i - \hat{\Delta x_i})^2 + (\Delta y_i - \hat{\Delta y_i})^2\right]} \tag{5}$$

where:

- n is the total number of sampled time points.
- $\Delta x_i, \Delta y_i$ represent the differences in the horizontal and vertical axes at the i^{th} time point.
- $\hat{\Delta x_i}, \hat{\Delta y_i}$ represent the mean of the differences in the horizontal axis and vertical axis, respectively at the i^{th} time point.

Lower RMSE values indicate better following stability and trajectory matching.

4) Response Time Delay (t_d): Measures the delay (t_d) between the leader's speed or directional change and the follower's corresponding adjustment. Find the time t_1 for the leader to change speed/direction, and record the time t_2 for the follower to react to the change. Finally, calculate the response time:

$$t_d = t_2 - t_1 \tag{6}$$

Shorter response times indicate better reactivity to leader movements.

IV. Results

A. Signal Detection Accuracy

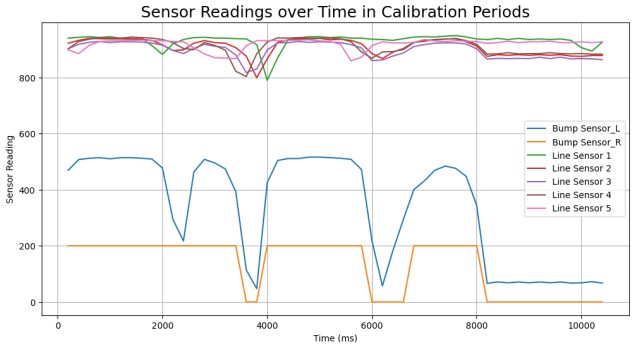

Fig. 4. Sensor Readings over Time in Calibration Periods

Fig. 4 shows the sensor readings during the calibration phase, where raw data from all seven infrared sensors were collected. The figure shows that the raw data range of the line sensors consistently exceeded 800, while the raw readings of the bump sensors were all below 600. Additionally, the line sensors exhibited similar variation patterns, with Line Sensor 1 and Line Sensor 5 showing relatively smaller fluctuations. The bump sensors also demonstrated consistent variation, but changes in the right-side bump sensor were triggered only when the left-side sensor readings fell below 200. Furthermore, both types of sensors experienced similar drops in readings before 4000 milliseconds and after 6000 milliseconds.

B. Position Deviation

TABLE I
Position Deviation Results of Three Sensor Configurations in Constant and Variable Speed Linear Motion

Sensors	Speed	Average ΔP	RMSE
Bump Sensors	Constant	(9.0795, 0.0676, 0.0114)	1.2421
	Variable	(10.1239, 0.1189, 0.0191)	1.4598
Line Sensors	Constant	(13.2996, 0.1739, 0.0183)	2.1677
	Variable	(14.4357, 0.2218, 0.0278)	2.1659
Bump & Line	Constant	(8.3427, 0.1674, 0.0138)	1.1289
	Variable	(8.4215, 0.0773, 0.0122)	1.1695

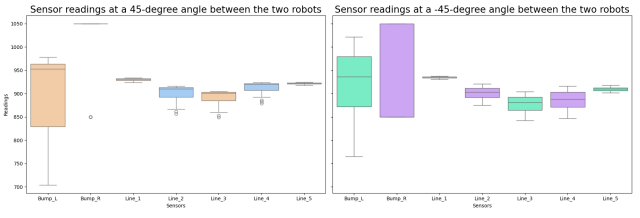

Fig. 5. Range of Sensor Readings in Sudden Turn Motion

Table I records the position deviation and RMSE results for the three sensor configurations in constant and variable speed linear motion. Fig. 5 demonstrates the sensor reading ranges during sudden-turn motions. It can be observed that the right bump sensor exhibits significant uncertainty during sudden turns, while the left bump sensor shows relatively consistent values across the two turning motions. Among the line sensors, DN1, DN3, and DN5 exhibit no significant differences, whereas DN2 and DN4 show variations. Specifically, DN2 has lower readings than DN4 during the 45-degree turn, whereas the opposite is true during the -45-degree turn.

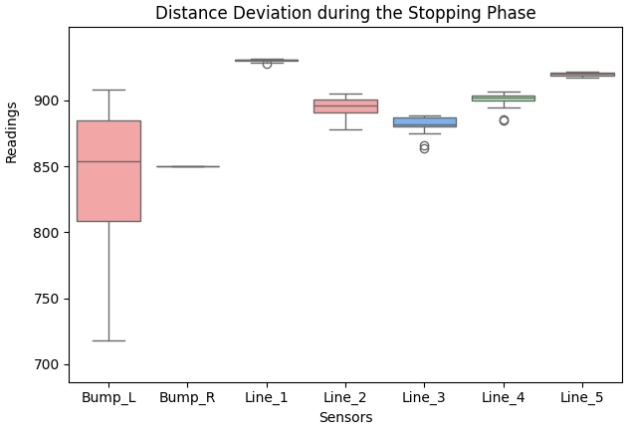

Fig. 6. Distance deviation at the stop of the experiment with 35 repetitions

Fig. 6 is a box plot showing the sensor data recorded by the follower robot when the leader robot stops were obtained through repeated experiments. During this phase, the distance between the two robots remains within the optimal range. The plot reveals that the readings of the Left Bump Sensor show significant variability when the robot stops, although most values are concentrated around 850. In contrast, the readings of the Right Bump Sensor consistently remain at 850. For the line sensors, the variability is minimal. Notably, DN3 has the lowest readings, DN2 and DN4 exhibit similar values, while DN1 and DN5 have the highest and most consistent readings.

C. Following Stability

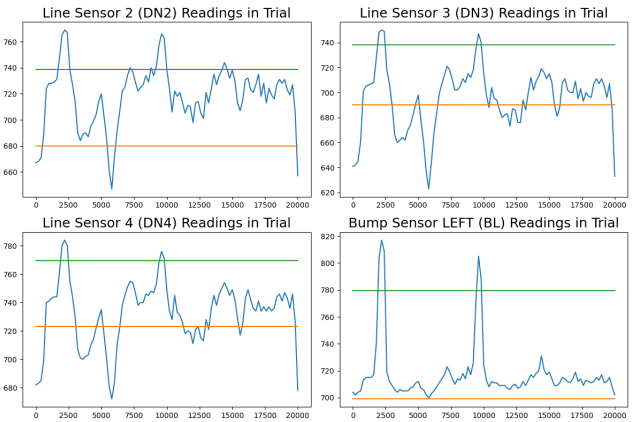

Fig. 7. Readings of Four Selected Sensors in the Experiment (The blue line represents real-time readings, while the green and orange lines indicate the experimentally determined optimal distance range.)

Fig. 7 plots the sensor readings during the sensor fusion experiment for constant speed linear motion. To align their range with the line sensor readings, the bump sensor readings were uniformly increased by 650. The total experiment duration was 20 seconds. From the figure, it can be observed that during the start phase, all sensor readings increased, and the robot transitioned to a following motion around 1000 milliseconds. In the first half of the experiment, the robot's following state was relatively

unstable, but it became more stable after 10,000 milliseconds. In the stopping phase, all sensor readings decreased. The green and orange lines represent the maximum and minimum readings corresponding to the optimal following distance range for each sensor. Furthermore, for most of the experimental duration, the robot remained within the optimal following distance range.

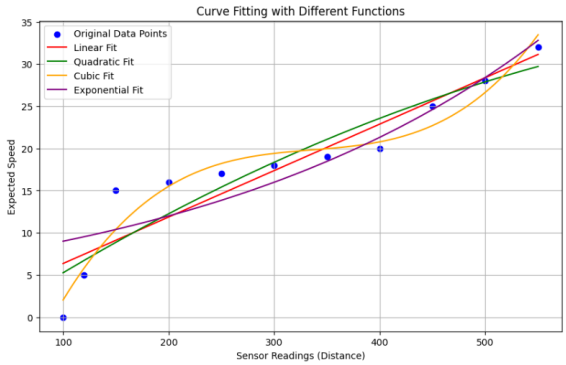

Fig. 8. Four Feasible Fitting Methods

Fig. 8 displays the comparison of fitting methods, where the cubic fit method aligns more closely with the original data points. While other fitting methods align more closely with a linear trend.

V. Discussion and Conclusion

In this study, BL, BR, DN1, DN2, DN3, DN4 and DN5 sensors on the Pololu 3pi+ robot are used to determine through experiments that multi-sensor combination can improve the tracking stability in Leader-Follower tasks. In addition, the experimental results also confirm that the optimal sensor combination is the left bump sensor and the middle three linear sensors, which support the Leader-Follower function and adapt to sudden turning.

This study commences with an investigation into the distinct characteristics inherent to each sensor, entailing the transmission and reception of data from individual sensors. Consequently, the sensors are subjected to a targeted screening and fusion process, with the objective of reducing the hardware requirements of the robot system. Additionally, the study validated the leader-follower performance under extreme turning scenarios based on the proposed hypotheses to enhance the robot's adaptability, with the leader's turning angle limited to a maximum of ±45 degrees. Thus, Fig. 5 highlights the importance of the DN2 and DN4 line sensors in turning scenarios.

The accuracy of signal detection is mainly evident in Fig. 4 and Fig. 7, where the data collection is continuous and reasonable, though there is a 200-millisecond gap in data acquisition during the startup phase. Therefore, the accuracy of signal acquisition can be calculated as **99%**. In both figures, data was sampled at 200-millisecond intervals to prevent data overflow. Additionally, these figures also demonstrate that the utilisation of a single sensor type is sufficient for the two robots to achieve the desired "leader-follower" linear motion. However, the optimisation of hardware requirements is also advantageous, as it reduces the burden on the hardware system and allows for the storage of a greater quantity of collected data, thereby facilitating the attainment of more precise experimental outcomes.

The position deviation was then assessed, and this study yielded 35 valid tracking movements through the utilisation of endpoint sampling. The distance between the two robots and the sensor readings were recorded at the point of cessation, which revealed that the left bump sensor exhibited considerable variability in the data it produced. However, the line sensor readings were relatively stable, which may be attributed to the follower's braking not being prompt, resulting in a consistently minimal stopping distance.

Validation of follow stability presents certain challenges. This study recorded sensor data during motion, as shown in Fig. 5 and Fig. 7. It is evident that sensor readings remained within the optimal following distance for most of the time, which aligns with the experimental hypothesis. Furthermore, when deviating from the optimal range, timely adjustments were made to maintain the following motion. Although PID parameter tuning was employed, Fig. 7 still shows that this following strategy exhibits significant fluctuations.

Additionally, time delay (t_d) can be observed in Fig. 7. After the stable following motion concludes, the sensor readings show a significant drop in the last two sampling intervals, indicating that the follower did not detect the leader's sudden stop in time. Therefore, it can be inferred that the time delay between the two robots is approximately 400 milliseconds, but the impact on the following performance is minimal.

In conclusion, this study conducted Leader-Follower tasks on the Pololu 3Pi+ robot. The results show that the combination of bump sensors and line sensors performs best in terms of position deviation and RMSE, and in scenarios involving sudden turns, the linear sensors DN2 and DN4 provided more stable detection. In addition, while machine learning was proposed and initially tested, it did not produce better results than current experiments. Therefore, future work may explore integrating advanced algorithms, such as adaptive PID or machine learning techniques, to further enhance the robustness and efficiency of Leader-Follower systems.

References

[1] "Vision-based leader-follower formations with limited information | IEEE Conference Publication | IEEE Xplore." https://ieeexplore.ieee.org/document/5152261.

[2] "Vision-Based Leader–Follower Formation Control of Multiagents With Visibility Constraints | IEEE Journals & Magazine | IEEE Xplore." https://ieeexplore.ieee.org/abstract/document/8269328?casa_token=2x-GrxJI65ycAAAAA:XA_On7N2YTjxF4PcFGzVmbSrpS8pNj4pZ0cu-KEnJSTDkz0oXJxYHxW3RNejAWjfxcQvDqmqxLg.

[3] M. Özcan, F. Aliew, and H. Görgün, "Accurate and precise distance estimation for noisy IR sensor readings contaminated by outliers," *Measurement*, vol. 156, p. 107633, May 2020.

[4] P. Wei and B. Wang, "Multi-sensor detection and control network technology based on parallel computing model in robot target detection and recognition," *Computer Communications*, vol. 159, pp. 215–221, June 2020.

[5] S. S. Rao and S. R. Desai, "Machine Learning based Traffic Light Detection and IR Sensor based Proximity Sensing for Autonomous Cars," July 2021.

[6] D. Sakai, H. Fukushima, and F. Matsuno, "Leader–Follower Navigation in Obstacle Environments While Preserving Connectivity Without Data Transmission," *IEEE Transactions on Control Systems Technology*, vol. 26, pp. 1233–1248, July 2018.

[7] "Pololu - 3pi+ 32U4 OLED Robot - Standard Edition (30:1 MP Motors), Assembled." https://www.pololu.com/product/4975.

[8] "Pololu - 5.5. Line and bump sensors." https://www.pololu.com/docs/0J83/5.5.